ISEIS

Journal of Environmental Informatics 39(2) 125-135 (2022)

Journal of Environmental Informatics

www.iseis.org/jei

Spatiotemporal Modelling of Groundwater Flow and Nitrate Contamination in An Agriculture-Dominated Watershed

M. Eryiğit[1] * and B. Engel[2]

[1] *Department of Environmental Engineering, Bolu Abant Izzet Baysal University, Bolu 14030, Turkey*
[2] *Department of Agricultural and Biological Engineering, Purdue University, West Lafayette, Indiana 47907, USA*

Received 10 March 2021; revised 15 July 2021; accepted 02 September 2021; published online 08 December 2021

ABSTRACT. In this study, both groundwater flow and nitrate transport were simulated in the Upper White River Watershed (Indiana, US) dominated by agricultural production. MODFLOW and MT3DMS were used for groundwater flow and contaminant transport modelling of the watershed under transient conditions. The input files for MODFLOW and MT3DMS were obtained by the GMS groundwater simulator. Model simulations were performed for 25 years between 1995 ~ 2019 with one-year intervals. Groundwater observation data (hydraulic heads and nitrate concentrations) for 1995 ~ 2013 and 2014 ~ 2019 were used for the model calibration and validation, respecttively. A heuristic optimization model based on the modified Clonal Selection Algorithm (a class of Artificial Immune Systems) was improved for calibration of the groundwater contaminant transport model. MODFLOW and MT3DMS were linked with the algorithm and run in MATLAB. Based on land use/cover, recharge and recharge nitrate concentrations were calibrated while other groundwater parameters (storage, porosity, longitudinal dispersivity, and denitrification rate coefficients) were calibrated for 7 aquifers. Furthermore, the models were run for different scenarios representing possible future conditions. The results demonstrated that the models performed well in terms of the fate and transport of nitrate in the Upper White River Watershed.

Keywords: nitrate contamination, groundwater contaminant transport, groundwater flow, modeling, agricultural watershed, heuristic optimization

1. Introduction

Water is vital for human and other living creatures. Water resources for drinking are quite limited in the world. Therefore, freshwater resources based on groundwater and surface water should be protected and managed properly. Recently, rapid human population growth and developing technology have caused decreasing water resources and increasing water pollution. Especially, misapplications of irrigation (unauthorized excessive consumption of groundwater), excessive usage of fertilizer and pesticides (including manure) are harmful to groundwater. The excessive use of fertilizer results in nitrate (NO_3) pollution of groundwater. Thus, public health can be affected by high NO_3 concentration in drinking water. This can cause serious health problems such as a blue baby syndrome for new-born babies as well as a gastric cancer for adults (Kapoor and Viraraghavan, 1997; Almasri, 2007; Ozturk and Goncu, 2017). Also, NO_3 is one of the ions causing water hardness. The World Health Organization (WHO) defines NO_3 pollution as over 50 mg/L concentration in groundwater for drinking (WHO, 1995).

In this context, there are several studies related to groundwater vulnerability-risk modelling and mapping (DRA-STIC-GIS, GOD, etc.) for NO_3 pollution. Engel et al. (1996) used DRASTIC, SEEPAGE, SPISP models and GIS for mapping groundwater vulnerability of NO_3 and pesticide pollution based on agricultural areas in Midwest America. Similarly, McLay et al. (2001), Sener et al. (2009), Firat Ersoy and Gultekin (2013), Chandoul et al. (2014), Eke et al. (2015), Arauzo (2017), Jang et al. (2017), Ramaraju and Veni (2017), and Zhai et al. (2017) applied DRASTIC-GIS, LU-IV, and HHRA (USEPA) models for mapping groundwater vulnerability-risk assessment of NO_3 and pesticide pollution caused by agricultural activities in watersheds. Groundwater vulnerability models show only present areas under risk against pollutants in watersheds. They are limited and cannot perform spatiotemporal estimation of contaminants in the groundwater. Instead, groundwater flow and contaminant transport models are used such as MODFLOW (McDonald and Harbaugh, 1988) and MT3DMS (Zheng and Wang, 1999). Birkinshaw and Ewen (2000), Molenat and Gascuel (2002), David (2003), Almasri and Kaluarachchi (2007), Orban (2008), Jiang and Somers (2009), Baalousha (2013), Wang et al. (2013), Psarropoulou and Karatzas (2014), and Noori et al. (2018) used SHETRAN, MODFLOW-MT3D, LEACHM, MODFLOW-MT3D, HFEMC-SUFT3D, numerical models (NFM, NTB and GIS groundwater), MODFLOW-MT3DMS, and ROM-MT3DMS for modeling the groundwater flow and NO_3 transport in the agricultural watersheds, respectively. Similarly, Zhang et al. (2019) used MODFLOW and MT3DMS model for the prediction of agriculture-related NO_3 contamination in

* Corresponding author. Tel.: +90-374-2541000/4860.
E-mail address: miraceryigit@hotmail.com (M. Eryiğit).

ISSN: 1726-2135 print/1684-8799 online
 Doi:10.3808/jei.202100470.

groundwater. Zhang et al. (2020) used HYDRUS-1D, MODFLOW and MT3DMS for modeling fertileization impacts on NO_3 leaching and groundwater contamination. Noori et al. (2020) developed the POD model linked to MT3DMS (POD-MT3DMS-Tool) for predicting NO_3 in aquifers. Ameur et al. (2021) used Susceptibility Index and MT3DMS to simulate pollution transport of NO_3 in the aquifer. Samadi-Darafshani et al. (2021) modeled aquifer flow and NO_3 contaminant transport and concentration in the aquifer by using MODFLOW and MT3D. A model calibration process was performed manually in most of these studies. Manual calibration causes a time loss and may not be reliable exactly (because there are numerous trial and error adjustments depending on number of parameters and it is almost impossible to test all trials and errors manually). Therefore, as an alternative to the related literature, this study aims at spatiotemporal modeling groundwater flow and NO_3 pollution in an agriculture-dominated watershed by using a heuristic optimization model based on artificial immune systems for groundwater model calibration (instead of manual calibration). The optimization model was developed to calibrate groundwater flow and groundwater contaminant transport model parameters such as riverbed conductivity, porosity, longitudinal dispersivity, denitrification rate, recharge concentration for a real groundwater system (case study). There is no another optimization model developed (linked with MODFLOW and MT3DMS) for calibrating these parameters simultaneously under transient conditions in the related literature. Recharge and recharge NO_3 concentrations were calibrated by considering land use/cover while storage, porosity, longitudinal dispersity and denitrification rate coefficients were calibrated for 7 aquifers in the watershed.

2. Materials and Methods

2.1. Study Area

The study area is the Upper White River Watershed (UWRW) in Indiana, US (Figure 1). Drainage area of the watershed is 7,044 km^2. Land use/cover of UWRW consists of 50.6% agricultural areas, 26.4% urban areas, 13.8% forest, 7.2% pasture, and 2% others (wetlands, barren lands, etc.) (Figure 2). The watershed includes 4 large reservoirs as well as the White River. Lowest and highest elevations of UWRW are 162.9 and 371.7 m, respectively (Figure 3). Mean annual precipitation is 1,093 mm, and maximum, minimum and mean daily temperatures are 36.1, –31.3, and 10.8 ºC (NCDC, 2010). In this study, groundwater divide (basin) was assumed to overlap/coincide with the surface watershed boundary. UWRW includes 11 aquifer types (Figure 4) (IDNR, 2011). However, 7 aquifer types were considered because some of them have small areas and are negligible. There are 775 registered pumping wells in UWRW.

2.2. Model Formulation

In this study, MODFLOW and MT3DMS were used for modelling groundwater flow and NO_3 transport in UWRW. The input files for MODFLOW and MT3DMS were obtained by the GMS groundwater simulator. Different parameters need to be calibrated for groundwater modelling such as recharge, storage coefficient, hydraulic conductivity, pumping rate, recharge and river concentration (Hill et al., 2000; Almasri and Kaluarachchi, 2007; Edet et al., 2014; Wohlgemuth, 2016; Noori et al., 2018). The modified clonal selection algorithm (Clonalg) was used as the heuristic optimization method for model calibration (Eryiğit, 2015). In order to simulate groundwater flow and NO_3 transport, MODFLOW and MT3DMS were used in conjunction with the algorithm in MATLAB.

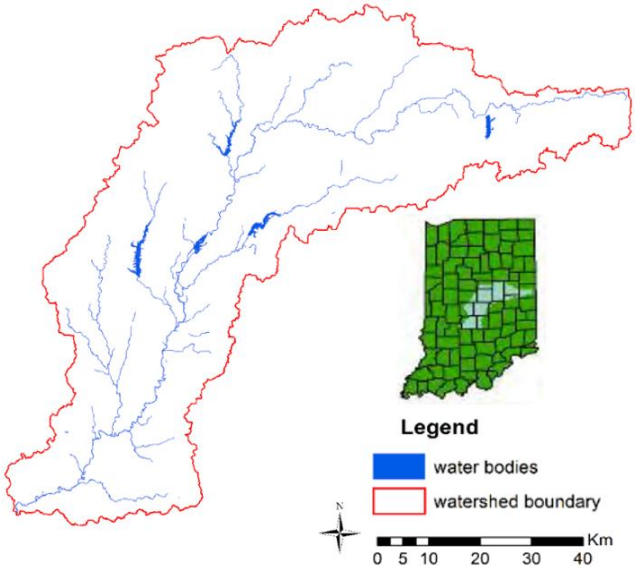

Figure 1. The study area (Upper White River Watershed).

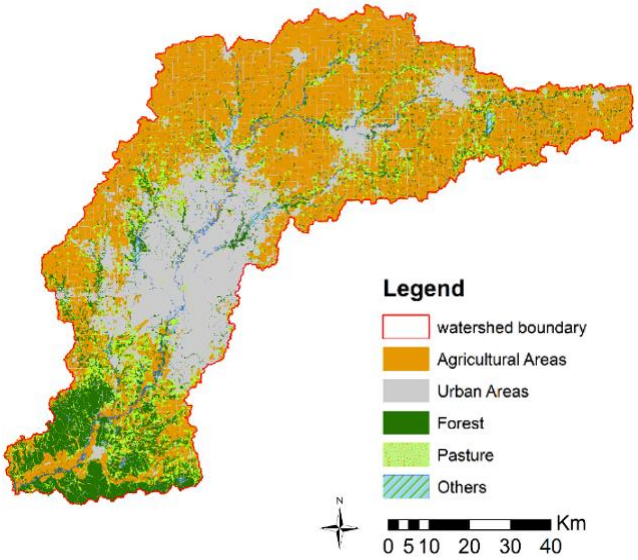

Figure 2. Land use/cover (2016) of the study area (UWRW) (MRLC, 2019).

2.2.1. Groundwater Flow Model

The partial-differential equation of the three-dimensional groundwater flow used in MODFLOW is as follows (McDonald and Harbaugh, 1988):

$$\frac{\partial}{\partial x}\left(K_{xx}\frac{\partial h}{\partial x}\right)+\frac{\partial}{\partial y}\left(K_{yy}\frac{\partial h}{\partial y}\right)+\frac{\partial}{\partial z}\left(K_{zz}\frac{\partial h}{\partial z}\right)+W=S\frac{\partial h}{\partial t} \quad (1)$$

where K_{xx}, K_{yy} and K_{zz} are hydraulic conductivity values along the x, y and z coordinate axes (L/T), h is the hydraulic head (L), W is the volumetric flux per unit volume representing sources and/or sinks of water, with $W < 0$ for flow out of the groundwater system, and $W > 0$ for flow into the system (T^{-1}), S is the specific storage of the porous material (L^{-1}), and t is time (T).

The groundwater flow model was created in GMS considering the main river (White River), 4 reservoirs and pumping wells (Figure 5). A two-dimensional one confined layer was assumed for the groundwater system of UWRW. A grid cell size of 500 × 500 m ($\Delta x = \Delta y = 500$ m) was used. The river package, CHD package and well package in GMS were used for the White River, the reservoirs and the pumping wells, respectively. USGS DEM raster data and surface water gage height data were used for water levels of the reservoirs, the river and bottom elevations of the riverbed.

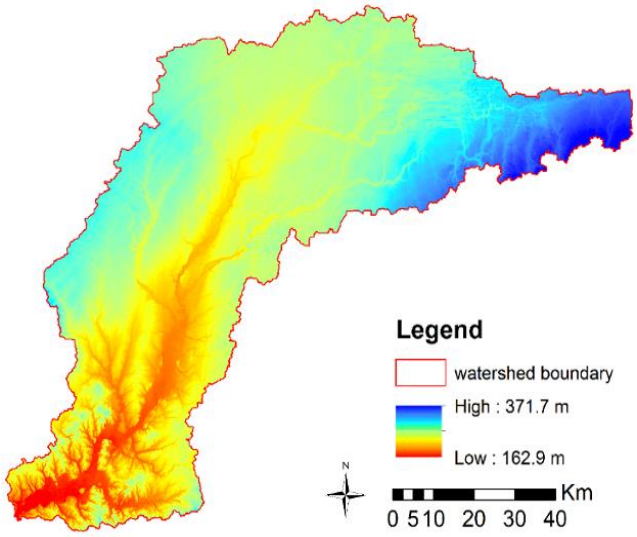

Figure 3. Elevations (DEM) of the study area (UWRW).

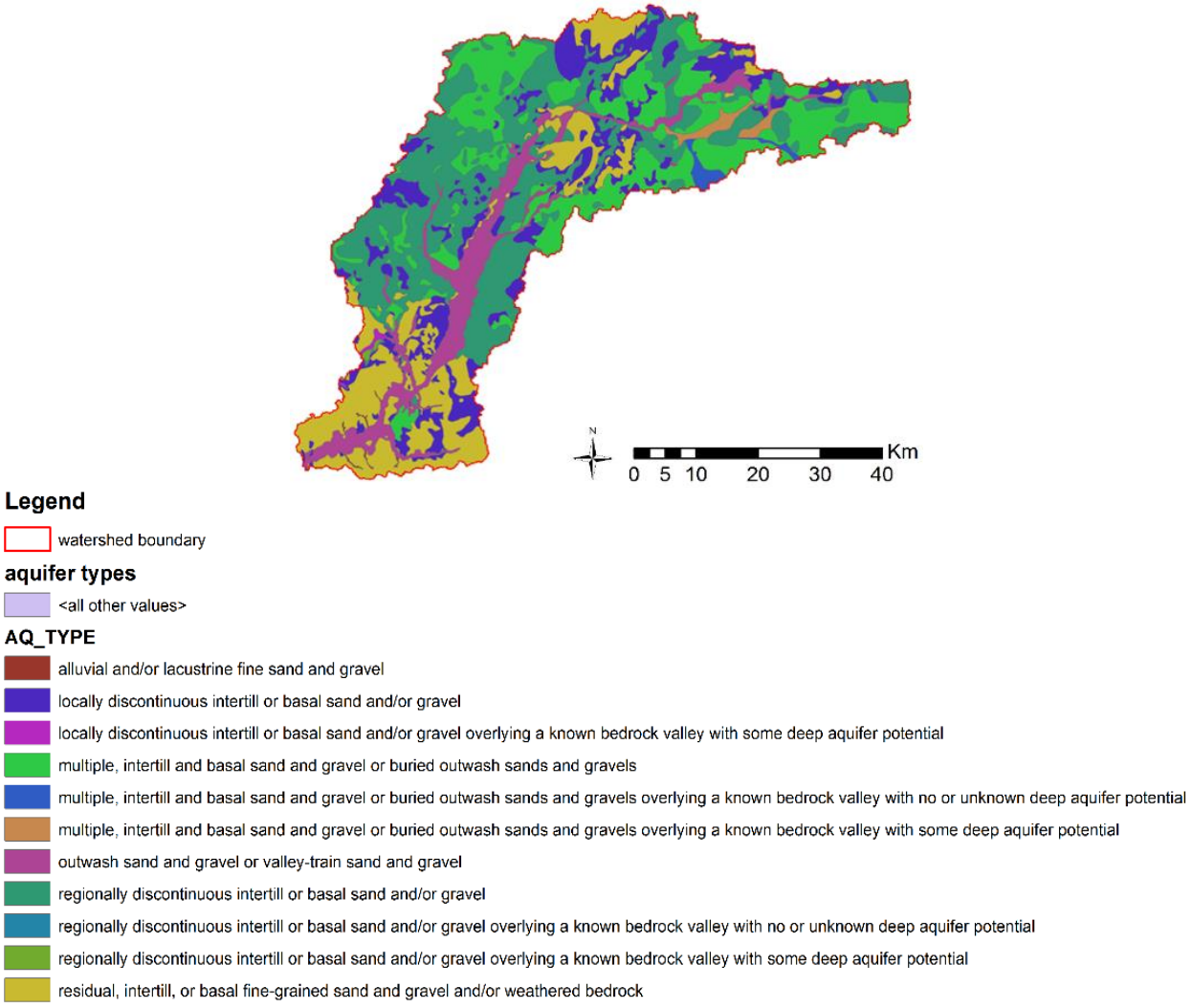

Figure 4. Aquifer types of UWRW.

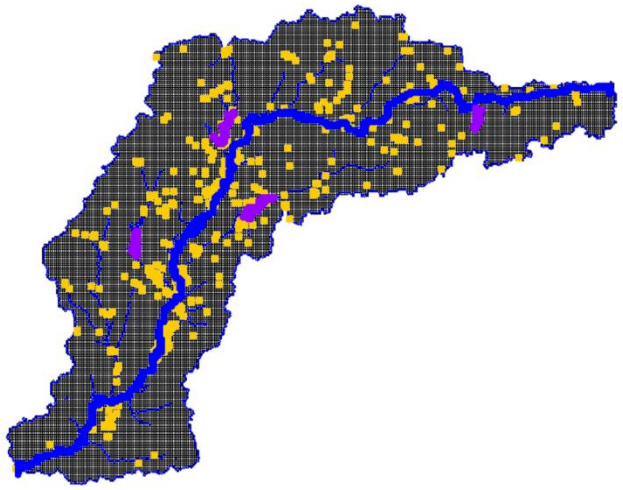

Figure 5. One-confined-layer groundwater model of UWRW in GMS (Yellow points are pumping wells).

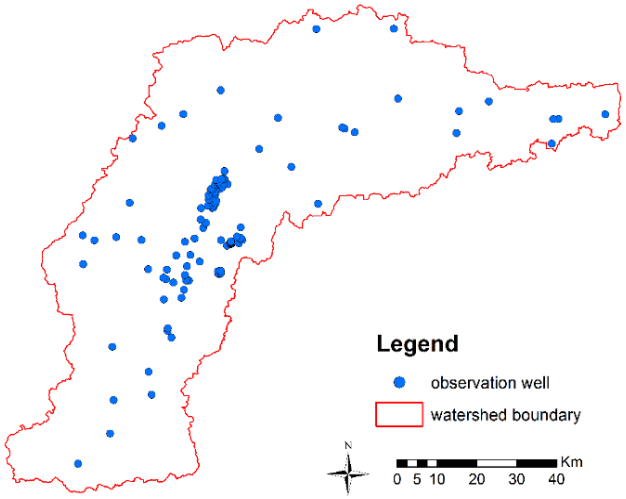

Figure 6. Locations of groundwater level observation wells in UWRW (1995 ~ 2019).

The aquifer transmissivity data were obtained from IDNR (2011). These data were interpolated by using Inverse Distance Weighting (IDW) to the entire watershed. According to land use/cover (Figure 2), four groundwater recharge regions (agriculture, urban, forest, and pasture) were considered for the recharge package. Evapotranspiration raster data were supplied from USGS (2019) for the evapotranspiration package. The time interval was selected as yearly (Δt = year) due to data gaps. Groundwater hydraulic head data (observed water levels, h) between 1995 ~ 2019 were collected from USGS. These data were used for model calibration (1995 ~ 2013) and validation (2014 ~ 2019). Observed heads in 1995 were interpolated by using IDW for starting heads of the groundwater basin. Locations of groundwater level observation wells in UWRW are given in Figure 6.

The optimization model for groundwater flow of the UWRW was coded and linked with MODFLOW 2005 in MATLAB 2018b. The flowchart of the optimization model is given in Figure 7 (Eryiğit, 2021). In brief, input files of the groundwater flow are generated for MODFLOW in GMS. MODFLOW is run in MATLAB by using random groundwater flow parameters created by modified Clonalg. The predicted and observed hydraulic heads are read and used for calculating the objective function. All groundwater flow parameters are cloned and mutated (matured) through the algorithm. After mutation process, MODFLOW is run again by using mutated parameters. Predicted and observed hydraulic heads are read and used again for calculating the objective function. The parameter series which have minimum objective function values (best individuals) are selected to enter the population. This loop proceeds until iteration reaches maximum number or difference between max and min objective function values in the population is less than an assigned error. Hence, the optimum model calibration can be obtained.

The objective function was minimized during model calibration by using the model predicted and the field observed values of h under transient conditions. The objective function of the model is as follows:

$$\text{minimize} \sum_{i=1}^{N_h}\left(\sum_{t=1}^{N_t}\left|h_{pred,i,t}-h_{obs,i,t}\right|\right) \tag{2}$$

where $h_{pred,i,t}$ is the i-th predicted hydraulic head at t-th time, $h_{obs,i,t}$ is the i-th observed hydraulic head at t-th time, N_h is the number of observed heads and N_t is the number of times (days, years, etc.). Storage coefficients of 7 aquifers and recharge coefficients of 4 groundwater recharge regions in the watershed, and riverbed conductivity were unknown parameters. These parameters were calibrated simultaneously by the optimization model.

2.2.2. Groundwater Contaminant Transport Model

The partial differential equation of the fate and transport of contaminants for the three-dimensional transient groundwater flow systems used in MT3DMS is as follows (Zheng and Wang, 1999):

$$R\theta\frac{\partial C}{\partial t}=\frac{\partial}{\partial x_i}\left(\theta D_{ij}\frac{\partial C}{\partial x_j}\right)-\frac{\partial}{\partial x_i}\left(\theta v_i C\right)$$
$$+q_s C_s-q_s^{'}C-\lambda_1\theta C-\lambda_2\rho_b\overline{C} \tag{3}$$

where C is dissolved concentration of the contaminant (M/L^3), t is time (T), θ is porosity of the subsurface medium (unitless), R is the retardation factor (unitless), $x_{i,j}$ is a distance along the respective Cartesian coordinate axis (L), $D_{i,j}$ is a hydrodynamic dispersion coefficient tensor (L^2/T), v_i is a seepage or linear pore water velocity (L/T), q_s is a volumetric flow rate per unit volume of aquifer representing fluid sources (positive) and sinks (negative) (T^{-1}), C_s is the concentration of the source or sink flux for the contaminant (M/L^3), $q_s^{'}$ is the rate of change in transient groundwater storage (T^{-1}), λ_1 is a first-order reaction rate for the dissolved phase (T^{-1}), λ_2 is a first-order reaction rate

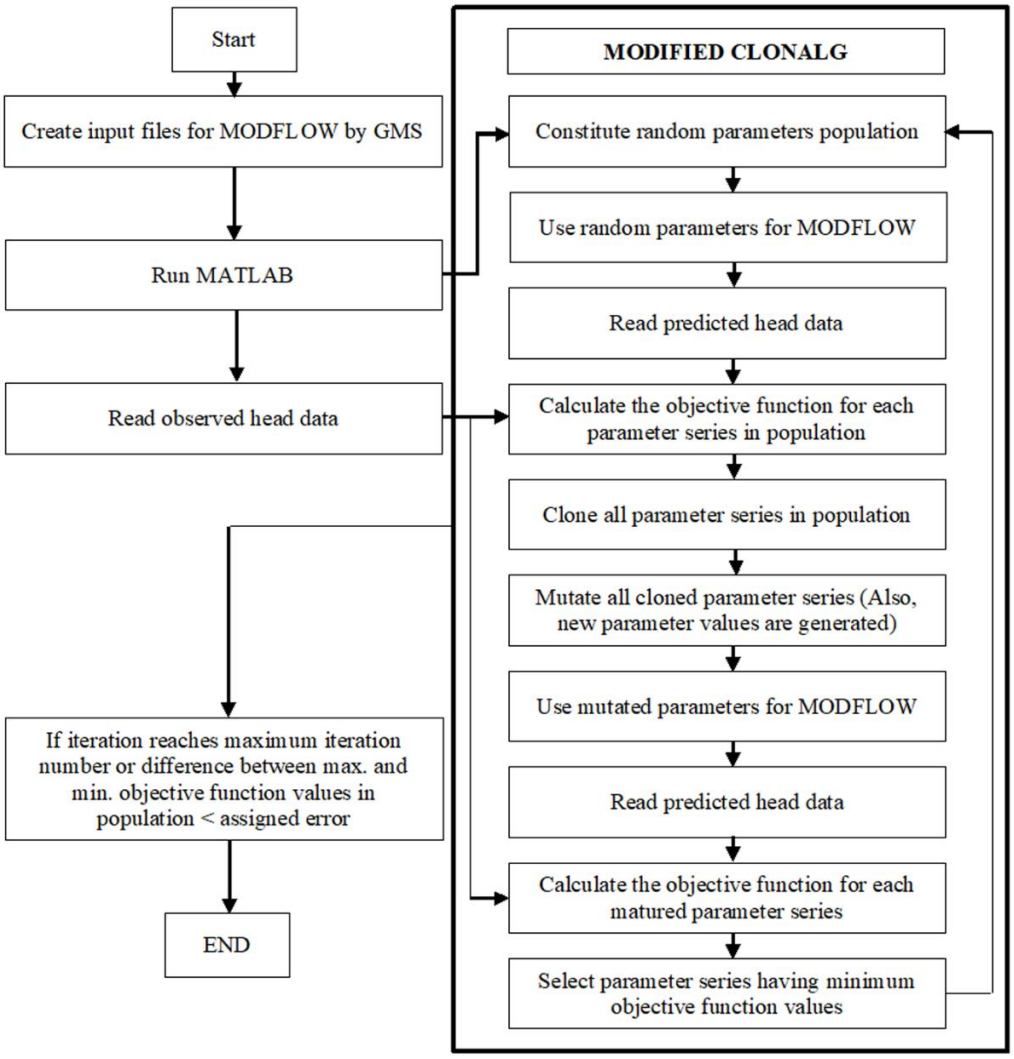

Figure 7. Flowchart of the optimization model for groundwater flow using modified Clonalg.

for the sorbed (solid) phase (T^{-1}), ρ_b is a bulk density of the subsurface medium (M/L), $\overline{C}$ is a concentration of the contaminant sorbed on the subsurface solids (M/M).

The hydraulic heads obtained from the groundwater flow model (MODFLOW) were used for the groundwater contaminant transport model (MT3DMS). The advection package, dispersion package, source/sink mixing package (river, reservoirs and recharge NO_3 concentrations) and chemical reaction package in GMS were used for spatiotemporal NO_3 contaminant (pollution) modelling. First-order irreversible kinetic reaction was selected, and sorption was assumed as none because NO_3 is a highly mobile species with little sorption in the groundwater (Meisinger and Randall, 1991; Birkinshaw and Ewen, 2000; Shamrukh et al., 2001). The ratio of transverse dispersivity to longitudinal dispersivity and molecular diffusion for NO_3 were assigned as 0.1 and 5×10^{-5} m^2/day, respectively (Frind et al., 1990; Gelhar et al., 1992). Recharge NO_3 concentrations were based on the 4 groundwater recharge regions according to land use/cover (agriculture, urban, forest, and pasture).

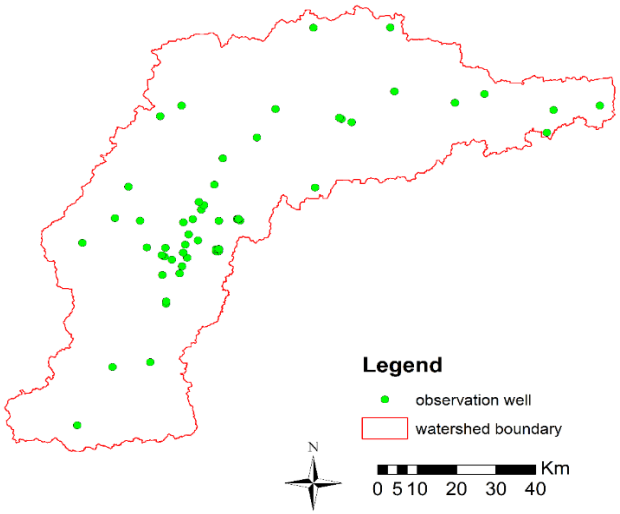

Figure 8. Locations of groundwater NO_3 concentration observation wells in UWRW (1995 ~ 2019).

NO_3 data of the groundwater, river and reservoirs between 1995 ~ 2019 were obtained from Water Quality Portal (WQP, 2019) and Heidelberg University. These data were used for model calibration (1995 ~ 2013) and validation (2014 ~ 2019). Observed concentrations in 1995 and years before 1995 (because of a lack of data) were interpolated by using the IDW for starting concentrations of the groundwater basin. The locations of groundwater NO_3 concentration observation wells in UWRW are shown in Figure 8. Similarly, the optimization model for groundwater contaminant transport of the UWRW was coded and linked with MT3DMS in MATLAB 2018b (Figure 9).

In summary, input files of the groundwater transport are generated for MT3DMS in GMS. MT3DMS is run in MATLAB by using random groundwater transport parameters created by modified Clonalg. Predicted and observed NO_3 concentrations are read and used for calculating the objective function. All groundwater transport parameter series are cloned and mutated (matured) through the algorithm. After mutation process, MT3DMS is run again by using mutated parameters. Predicted and observed NO_3 concentrations are read and used again for calculating the objective function. The groundwater transport parameters series which have minimum objective function values (best individuals) are selected to enter the population. The objective function was minimized during model calibration by using the model predicted and the field observed values of C under transient conditions. The objective function of the model is as follows:

$$\text{minimize} \sum_{i=1}^{N_c}\left(\sum_{t=1}^{N_t}\left|C_{pred,i,t}-C_{obs,i,t}\right|\right) \quad (4)$$

where $C_{pred,i,t}$ is the i-th predicted concentration at t-th time, $C_{obs,i,t}$ is the i-th observed concentration at t-th time, N_c is the number of observed concentrations and N_t is the number of times (days, years, etc.). Porosity, longitudinal dispersivity, and denitrification rate coefficients of 7 aquifers, and recharge concentrations of 4 groundwater recharge regions in the watershed were unknown parameters. These parameters were calibrated simultaneously by the optimization model.

2.2.3. Scenarios

After calibration and validation of the groundwater flow and contaminant transport models, three scenarios were modeled as follows: (1) Flow rates of pumping wells are doubled (double withdrawal). This scenario was carried out for estimating variation of hydraulic heads in the entire watershed after 25 years, while flow rates of pumping wells are doubled (represents increasing groundwater use). (2) Recharge concentration of agricultural areas is multiplied 10 times. This scenario was carried out for estimating variation of NO_3 concentrations in the entire watershed after 25 years, while recharge concentration of agricultural areas is multiplied 10 times and also pasture areas are turned into agricultural fields (represents increasing agricultural activities). (3) Combination of scenarios 1 and 2. This scenario is that flow rates of pumping wells are doubled while recharge concentration of agricultural areas is multiplied 10 times and pasture areas are turned into agricultural fields.

3. Results and Discussion

3.1. Results of UWRW Groundwater Flow Model

Calibrated model parameters, calibration and validation results are given in Table 1 and Table 2, respectively. Riverbed thickness was assumed as 0.305 m in the calibration of $K_{riverbed}$ (Yager, 1993). As can be seen in Table 1, $R_{pasture}$ (recharge from pasture) was higher than recharge for other land uses ($R_{agriculture}$, R_{urban}, and R_{forest}). Herbaceous/woody wetlands were included in pasture areas while calibrating recharges of land use/cover. Hence, it is reasonable that $R_{pasture}$ is high.

Hydraulic heads at the beginning (1995) and end (2019) of the simulation are illustrated in Figures 10a and b. There was a remarkable drop of hydraulic head (mean drop is 6.2 m, varying between 0 and 56.9 m) especially around the outlet of the watershed during the simulation (for 25 years). This drop occurred due to increasing pumping discharges (flow rates) and increasing numbers of pumping wells during 25 years and low R_{forest}. On the other hand, the groundwater head (hydraulic head) increased (mean rise is 18.9 m, varying between 1.5×10^{-5} and 68.6 m) throughout the rest of the watershed in general after 25 years. In this part of watershed, the groundwater is fed by the four big lakes in addition to a precipitation recharge (Figures 1 and 5). Owing to these lakes, the groundwater level could have been maintained against withdrawals by the pumping wells. The results indicate that there is a huge conflict between pumping wells and recharges in the UWRW throughout 25 years. Also, the balance of recharge and evapotranspiration was an important factor for variation of hydraulic heads.

MAE and RMSE of model calibration for the groundwater flow (difference between simulated and observed hydraulic heads) were less than 10% of the domain variation (±10 m) as suggested by Mandle (2002) (Table 2). Also, MAE for model validation was less than 10 m. Therefore, it can be said that the groundwater flow model was appropriately calibrated and validated. According to USGS data, the groundwater system of the UWRW was entirely assumed as a two-dimensional one confined layer to simplify the model. However, there are some exceptional unconfined layers in the study area. Thus, the MAE and RMSE results of the calibration and validation might have been affected negatively. Also, the results could be improved by applying a smaller grid cell size such as 100 × 100 m to the study area (in terms of model accuracy) (A grid cell size of 500 × 500 m was used in the study). But, it makes the model difficult and needs to more observation data.

3.2. Results of UWRW Groundwater Contaminant Transport Model

Calibrated model parameters, calibration and validation results are given in Table 3 and Table 4, respectively. As can be seen in Table 3, agricultural areas had the highest recharge NO_3 concentration while the forest areas have the second highest recharge concentration among the land covers. The NO_3 concentrations at the beginning (1995) and end (2019) of the simula-

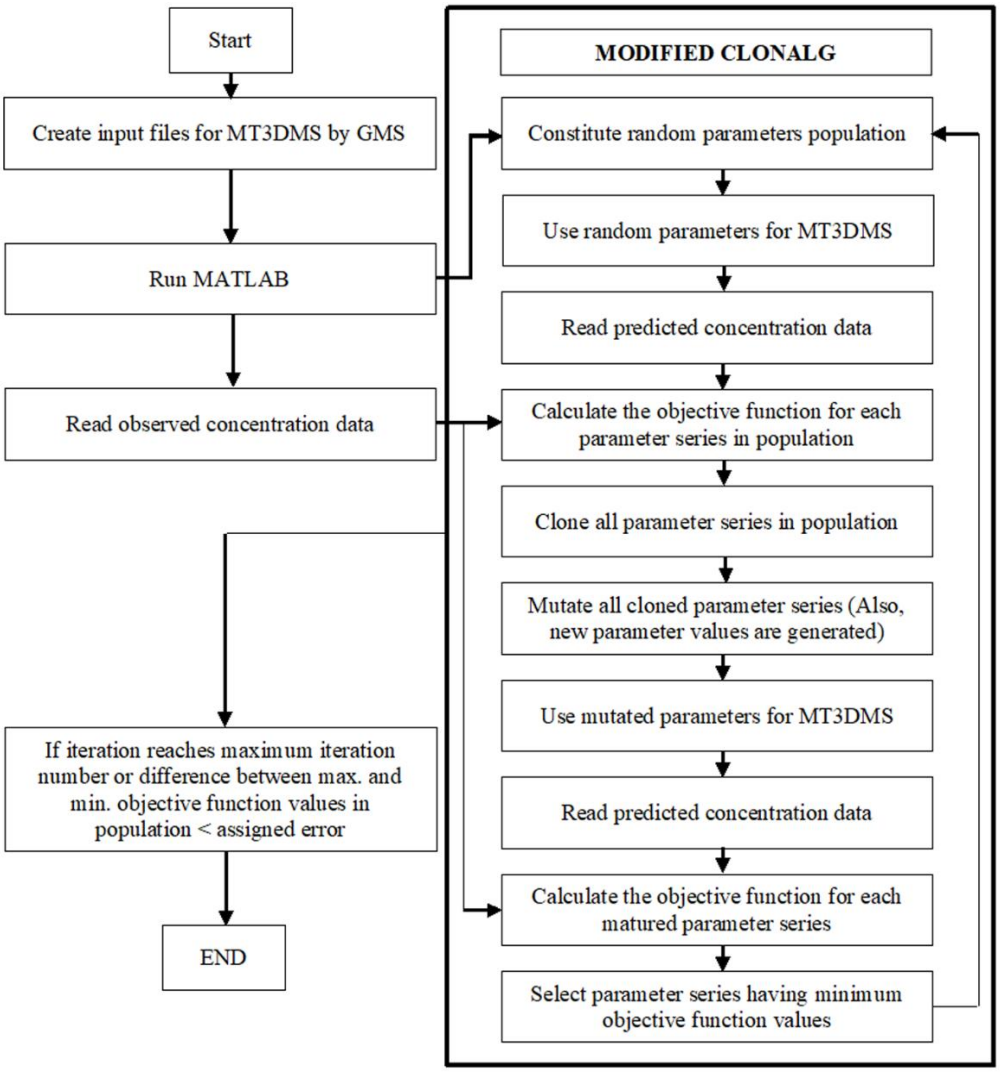

Figure 9. Flowchart of the optimization model for groundwater contaminant transport using modified Clonalg.

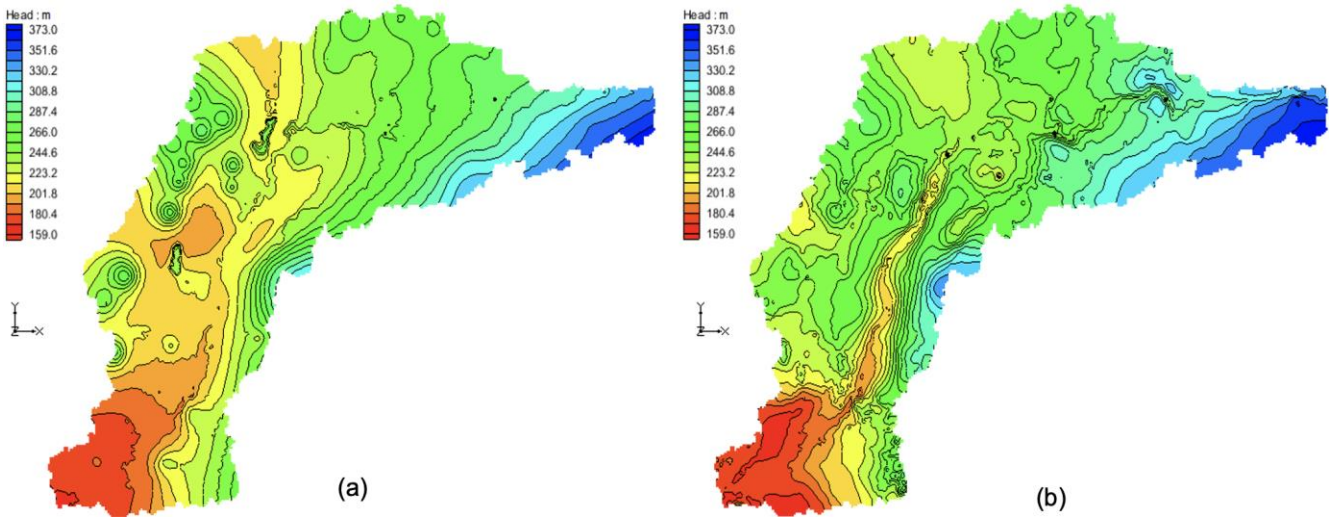

Figure 10. Simulated hydraulic heads in (a) 1995, and (b) 2019.

Table 1. Calibrated Groundwater Flow Parameters for the Optimization Model

Storage coefficients of aquifers (unitless)							Recharges of landuse/cover (m year^{-1})				Riverbed conductivity (m year^{-1})
S_1	S_2	S_3	S_4	S_5	S_6	S_7	$R_{agriculture}$	R_{urban}	R_{forest}	$R_{pasture}$	$K_{riverbed}$
0.2	0.2	0.2	0.2	0.2	0.2	0.2	0.66	0.94	0.62	1.18	281.5

Table 2. Calibration and Validation Results of Groundwater Flow Model

Calibration (1995 ~ 2013)		Validation (2014 ~ 2019)		N_{calib}	N_{valid}
MAE	RMSE	MAE	RMSE		
4.9 m	7.5 m	9.8 m	15.4 m	671	255

Table 3. Calibrated Groundwater Transport Parameters for the Optimized Model

Porosity (Unitless)		Longitudinal Dispersivity (m)		Denitrification Rate (year^{-1})		Recharge conc. of landuse/cover (mg/L)	
P_1	0.90	D_1	0.104	DR_1	0.006	$RC_{agriculture}$	0.12
P_2	0.17	D_2	0.392	DR_2	0.083	RC_{urban}	0.02
P_3	0.53	D_3	0.415	DR_3	0.362	RC_{forest}	0.11
P_4	0.82	D_4	0.272	DR_4	0.011	$RC_{pasture}$	0.01
P_5	0.10	D_5	0.354	DR_5	0.420		
P_6	0.89	D_6	0.096	DR_6	0.009		
P_7	0.57	D_7	0.189	DR_7	0.047		

Table 4. Calibration and Validation Results of Groundwater Transport Model

Calibration (mg/L) (1995 ~ 2013)		Validation (mg/L) (2014 ~ 2019)		N_{calib}	N_{valid}
MAE	RMSE	MAE	RMSE		
1.69	2.06	4.24	4.81	1235	390

tion are illustrated in Figure 11. While comparing Figures 2 and 11, the high predicted NO_3 concentrations in the groundwater around areas consisting of both forest and agriculture (around the outlet of the watershed) and calibrated recharge concentrations of these areas (higher than urban and pasture) overlap. These results were because fertilizers/manures were the main sources of NO_3 contamination in the agricultural watershed.

MAE and RMSE of model calibration for the groundwater contaminant transport (difference between simulated and observed NO_3 concentrations) were less than a threshold value of 10% of NO_3 variation (10 mg/L) as suggested by Noori et al. (2018) (Table 4). Also, MAE and RMSE of model validation were less than 10 mg/L. Therefore, it can be inferred that the groundwater contaminant transport model was properly calibrated and validated. Moreover, the results are in accord with the integrated aquifer vulnerability map of the UWRW created by Jang et al. (2017).

The groundwater modeling of the UWRW was performed under a constant land use/cover (Figure 2). However, the land use/cover in the watershed changed slightly during 25 years. This influenced both recharge and recharge NO_3 concentration, so that the MAE and RMSE results of the calibration and validation could have been affected negatively. Considering a change of the land use/cover, the groundwater of the watershed can be represented and simulated much better by the model.

3.3. Results of Scenarios

Simulated hydraulic heads and NO_3 concentrations in scenarios 1, 2, and 3 are illustrated in Figures 12, 13, and 14. According to scenario 1, mean drop of hydraulic head in the entire watershed after 25 years is 1.3 m (head drops vary between 0 and 78.7 m) in comparison with simulation head results of 2019. According to scenario 2, the mean increase of NO_3 concentration in the entire watershed after 25 years is 0.15 mg/L (increases of concentration vary between 0 and 7.9 mg/L) in comparison with simulation NO_3 results of 2019. According to scenario 3, the mean increase of NO_3 concentration in the entire watershed after 25 years is 0.11 mg/L (increases of concentration vary between 0 and 5.6 mg/L) in comparison with simulation NO_3 results of 2019.

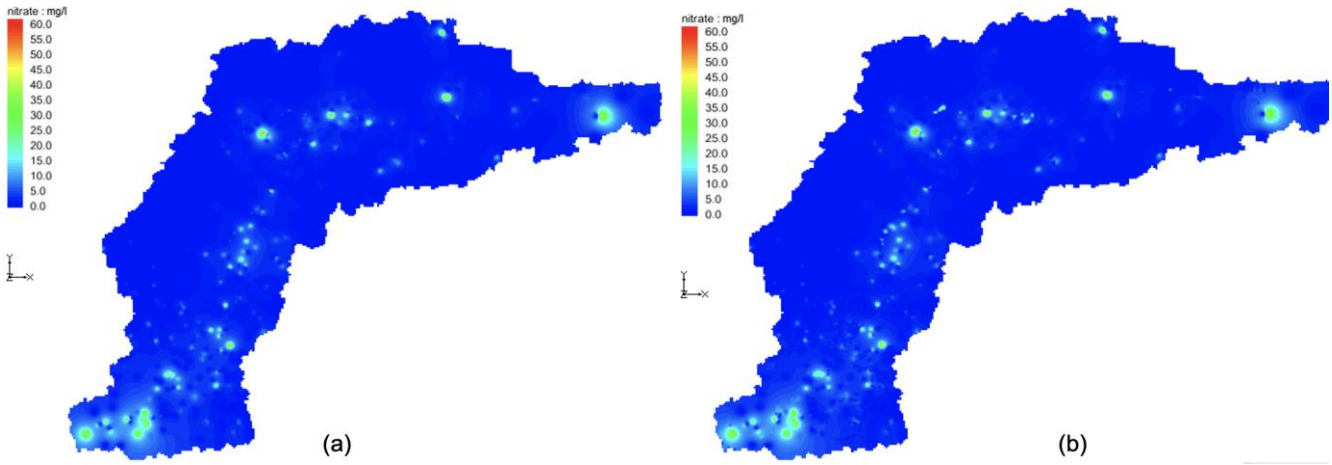

Figure 11. Simulated NO_3 concentrations in (a) 1995, and (b) 2019.

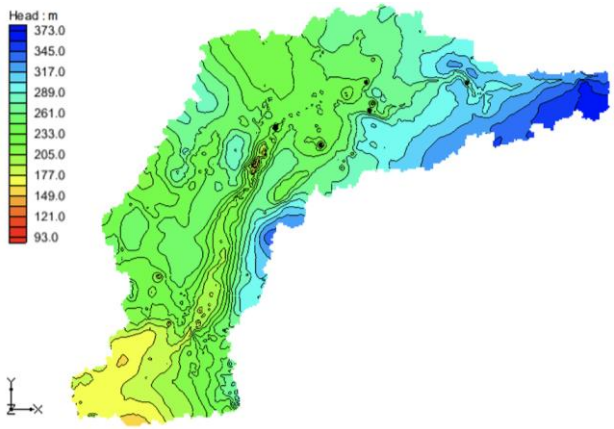

Figure 12. Simulated hydraulic heads in Scenario 1.

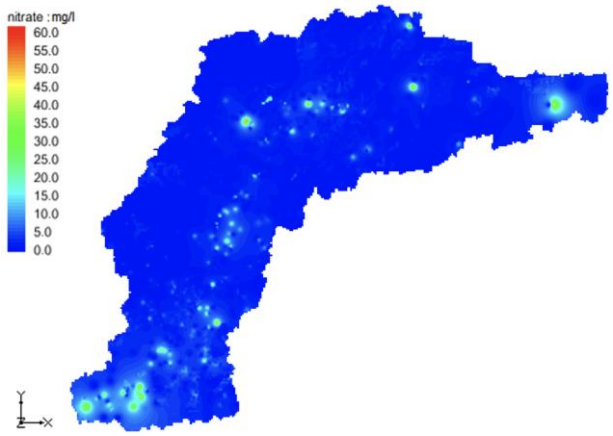

Figure 13. Simulated NO_3 concentrations in Scenario 2.

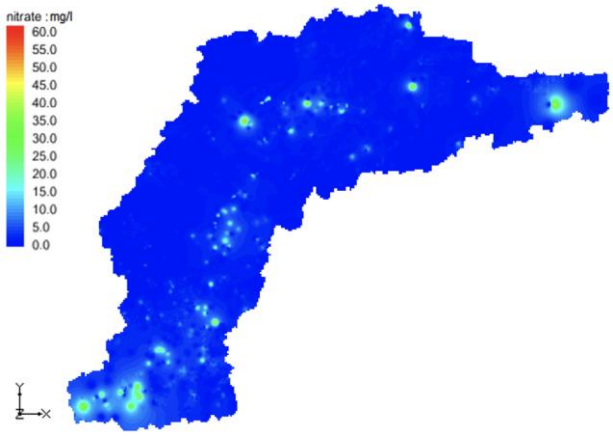

Figure 14. Simulated NO_3 concentrations in Scenario 3.

Although low mean head drop (1.3 m) and low mean increase of NO_3 concentration (0.15 and 0.11 mg/L) throughout the entire watershed, significant hydraulic head drops and increases of NO_3 concentration were seen of up to 78.7 m and 7.9 mg/L, respectively. It indicates that some parts of the study area may be vulnerable based on increasing irrigation and agricultural land use. Therefore, the obtained results may be considerable for agricultural policies in the watershed.

4. Conclusions

In this study, spatiotemporal groundwater flow and NO_3 transport models of the UWRW, which is an agriculture dominated watershed, were performed for 25 years. During the model calibration, numerous trial and error adjustments should be carried out to find the best model parameters and corresponding results. In order to facilitate this task, the optimization model with modified Clonalg (Eryiğit, 2021) was used instead of manual calibration (it was improved for the groundwater contaminant transport model in this study). There were many parameters required for the calibration such as recharge, recharge concentration, storage, porosity, longitudinal dispersivity, denitrification rate and riverbed conductivity in the study. The modified Clonalg was used for the first time to calibrate these parameters in a real groundwater system. In the related literature, these parameters were calibrated manually. Within this study, the improved optimization model makes the model calibration easier and more reliable (because all trials and errors can be performed/tested by the algorithm for obtaining an optimum calibration). The results showed that calibration and validation of the groundwater flow and transport models were acceptable according to the related literature (Mandle, 2002; Noori et al., 2018). Thus, it can be said that the optimization model is applicable and can be used for groundwater model calibration in future studies.

An aquifer vulnerability map of the UWRW for NO_3 was performed by using DRASTIC in the related literature (Jang et al., 2017), but it cannot simulate spatiotemporal variations of the flow and concentration in the groundwater. With this study, transient groundwater flow and contaminant transport models for the UWRW according to the different scenarios were applied. Thanks to this, the situations were able to be predicted under excessive groundwater use and agricultural activities. According to the three scenarios, considerable drops of hydraulic head and increases of NO_3 concentration in the groundwater would occur. Also, how the model responds to differrent independent variables (recharge concentration and pump flow rate) was seen. However, some uncertainty analysis (Monte Carlo, etc.) could be implemented for future studies. The study may provide guidance in terms of groundwater consumption and NO_3 pollution of the UWRW for future scenarios and future agricultural policies in the watershed.

Acknowledgements. This study was performed during the period the author was at Purdue University. The author thanks Prof. Dr. Bernard Engel for his acceptance as a visiting scholar at Purdue University. Also, the author thanks The Scientific and Technological Research Council of Turkey (TUBITAK) for the financial support (No:1059B 191800383).

References

Almasri, M.N. (2007). Nitrate contamination of groundwater: A conceptual management framework. *Environ. Impact Assess Rev.*, 27(3),

220-242. https://doi.org/10.1016/j.eiar.2006.11.002
Almasri, M.N. and Kaluarachchi, J.J. (2007). Modeling nitrate contamination of groundwater in agricultural watersheds. *J. Hydrol.*, 343, 211-229. https://doi.org/10.1016/j.jhydrol.2007.06.016
Ameur, M., Aouiti, S., Hamzaoui-Azaza, F., Cheikha, L.B. and Gueddari, M. (2021). Vulnerability assessment, transport modeling and simulation of nitrate in groundwater using SI method and modfow-MT3DMS software: case of Sminja aquifer, Tunisia. *Environ. Earth Sci.*, 80(6), 1-16. https://doi.org/10.1007/s12665-021-09491-z
Arauzo, M. (2017). Vulnerability of groundwater resources to nitrate pollution: A simple and effective procedure for delimiting Nitrate Vulnerable Zones. *Sci. Total Environ*., 575, 799-812. https://doi.org/10.1016/j.scitotenv.2016.09.139
Baalousha, H. (2013) *Ruataniwha Basin Nitrate Transport Modelling*. Hawkes Bay Regional Council, Environmental Management Group Technical Report, EMT 13/06, HBRC Plan Number 4470.
Birkinshaw, S.J. and Ewen, J. (2000). Modelling nitrate transport in the Slapton wood catchment using SHETRAN. *J. Hydrol.*, 230(1-2), 18-33. https://doi.org/10.1016/S0022-1694(00)00173-6
Chandoul, I.R., Bouaziz, S. and Dhia, H.B. (2014). Groundwater vulnerability assessment using GIS-based DRASTIC models in shallow aquifer of Gabes North (South East Tunisia). *Arab. J. Geosci*., 8(9), 7619-7629. https://doi.org/10.1007/s12517-014-1702-6
David, W. (2003). *Groundwater Flow And Contaminant Transport Model: Village of Greely And Surrounding Area*. Ottawa, Ontario.
Edet, A., Abdelaziz, R., Merkel, B., Okereke, C. and Nganje, T. (2014). Numerical Groundwater Flow Modeling of the Coastal Plain Sand Aquifer, Akwa Ibom State, SE Nigeria. *J. Water Resource Prot.*, 6, 193-201. https://doi.org/10.4236/jwarp.2014.64025
Eke, D.R., Opara A.I., Inyang G.E., Emberga T.T., Echetama H.N., Ugwuegbu, C.A., Onwe, R.M., Onyema, J.C. and Chinaka J.C. (2015). Hydrogeophysical evaluation and vulnerability assessment of shallow aquifers of the upper Imo river basin, Southeastern Nigeria. *Am. J. Environ. Prot*., 3(4), 125-136. https://doi: 10.12691/env-3-4-3
Engel, B., Navulur, K., Cooper, B. and Hahn, L. (1996). Estimating groundwater vulnerability to nonpoint source pollution from nitrates and pesticides on a regional scale. *HydroGIS 96: Application of Geographic Information Systems in Hydrology and Water Resources Management* (Proceedings of the Vienna Conference, April 1996), lAHSPubl. no. 235.
Eryiğit, M. (2015). Cost optimization of water distribution networks by using artificial immune systems. *J. Water Supply Res. T*., 64(1), 47-63. https://doi.org/10.2166/aqua.2014.031
Eryiğit, M. (2021). Estimation of parameters in groundwater modelling by modified Clonalg. *J. Hydroinformatics*, 23 (2), 298-306. https://doi.org/10.2166/hydro.2021.139
Firat Ersoy, A. and Gultekin, F. (2013) DRASTIC-based methodology for assessing groundwater vulnerability in the Gümüşhacıköy and Merzifon basin (Amasya, Turkey). *Earth Sci. Res. J*., 17(1), 33-40.
Frind, E., Duynisveld, W., Strebel, O. and Boettcher, J. (1990). Modeling of multicomponent transport with microbial transformation in ground water: the Fuhrberg case. *Water Resour. Res.*, 26(8), 1707-1719. https://doi.org/10.1029/WR026i008p01707
Gelhar, L.W., Welty, C. and Rehfeldt, K. (1992). A critical review of data on field-scale dispersion in aquifers. *Water Resour. Res.*, 28 (7), 1955-1974. https://doi.org/10.1029/92WR00607
Hill, M.C., Banta, E.R., Harbaugh, A.W. and Anderman, E.R. (2000). *Geological Survey Modular Groundwater Model-User Guide to the Observation, Sensitivity, and Parameter-Estimation Processes and Three Post-Processing Programs*. US Geological Survey Open-File Report 00-184. https://doi.org/10.3133/ofr00184
IDNR (2011). Indiana Department of Natural Resources, https://www.in.gov/dnr/ (accessed September 22, 2020)
Jang, W.S., Engel, B., Harbor, J. and Theller, L. (2017). Aquifer vulnerability assessment for sustainable groundwater management using DRASTIC. *Water*, 9(10), 792. https://doi.org/10.3390/w910 0792
Jiang, Y. and Somers, G. (2009). Modeling effects of nitrate from non-point sources on groundwater quality in an agricultural watershed in Prince Edward Island, Canada. *Hydrogeol. J.*, 17, 707-724. https://doi.org/10.1007/s10040-008-0390-2
Kapoor, A. and Viraraghavan, T. (1997). Nitrate removal from drinking water-Review. *J. Environ. Eng*., 123(4), 371-380. https://doi.org/101061/(ASCE)0733-9372(1997)123:4(371)
Mandle, R.J. (2002). *Groundwater modeling guidance*. Michigan Dept of Environmental Quality, GMP.
Meisinger, J.J., and Randall, G.W. (1991). *Estimating N budgets for soil crop systems.* Managing N for Groundwater Quality and Farm Profitability. Soil Science Society of America, Madison Wisconsin, pp 85-124. https://doi.org/10.2136/1991.managingnitrogen.c5
McDonald, M.G. and Harbaugh, A.W. (1988). *A modular three-dimensional finite-difference groundwater flow model.* US Geological Survey Open File Report, 83-875, chap. A1, 586 p.
McLay, C.D.A., Dragten, R., Sparling, G. and Selvarajah, N. (2001). Predicting groundwater nitrate concentrations in a region of mixed agricultural land use: a comparison of three approaches. *Environ. Pollut.*, 115, 191-204. https://doi.org/10.1016/S0269-7491(01)00111-7
Molenat, J. and Gascuel Odoux, C. (2002). Modelling flow and nitrate transport in groundwater for the prediction of water travel times and of consequences of land use evolution on water quality. *Hydrol. Process*., 16, 479-492. https://doi.org/10.1002/hyp.328
MRLC (2019). Multi-Resolution Land Characteristics (MRLC) Consortium. https://www.mrlc.gov/data/nlcd-2016-land-cover-conus/
NCDC (2010). National Climatic Data Center, https://www.ncdc.noaa.gov/ (accessed October 3, 2020)
Noori, R., Dodangeh, M., Berndtsson, R., Hooshyaripor, F., Adamowski, J.F., Javadi, S. and Baghvand, A. (2018). A novel model for simulation of nitrate in aquifers. *Hydrol. Earth Syst. Sci. Discuss.*, 2018, 1-21. https://doi.org/10.5194/hess-2018-222.
Noori, R., Hooshyaripor, F., Javadi, S., Dodangeh, M., Tian, F., Adamowski, J.F., Berndtsson, R., Baghvand, A. and Klöve, B. (2020). PODMT3DMS-Tool: proper orthogonal decomposition linked to the MT3DMS model for nitrate simulation in aquifers. *Hydrogeol. J*., 28, 1125-1142. https://doi.org/10.1007/s10040-020- 02114-0
Orban, P. (2008). *Solute transport modelling at the groundwater body scale: Nitrate trends assessment in the Geer basin (Belgium)*. PhD Thesis, Liege University, Wallonia, Belgium
Ozturk, E.T. and Goncu, S. (2017). Removal of nitrate from groundwater by using algae culture. *Ege J. Fish. Aquat. Sci*., 34(4), 463-467. https://doi.org/10.12714/egejfas.2017.34.4.15
Psarropoulou, E.T. and Karatzas, G.P. (2014). Pollution of nitrates-contaminant transport in heterogeneous porous media: A case study of the coastal aquifer of Corinth, Greece. *Glob. NEST J*., 16(1), 9-23. https://doi.org/10.30955/gnj.001209
Ramaraju, A.V. and Veni, K.K. (2017). Groundwater vulnerability assessment by DRASTIC method using GIS. *SSRG Int. J. Geoinf. Geol. Sci*., 4(2), 6-13, https://doi.org/10.14445/23939206/IJGGS-V4I 2P101
Samadi-Darafshani, M., Safavi, H.R., Golmohammadi, M.H. and Rezaei, F. (2021). Assessment of the management scenarios for ground water quality remediation of a nitrate-contaminated aquifer. *Environ. Monit. Assess*., 4(193),190-206. https://doi.org/10.1007/s10661021 -08978-3
Shamrukh, M., Corapcioglu, M., Hassona, F. (2001). Modeling the effect of chemical fertilizers on ground water quality in the Nile Valley Aquifer, Egypt. *Ground Water*, 39 (1), 59-67. https://doi.org/10.1111/j.1745-6584.2001.tb00351.x
Sener, E., Sener, S. and Davraz, A. (2009). Assessment of aquifer vulnerability based on GIS and DRASTIC methods: a case study of the Senirkent-Uluborlu Basin (Isparta, Turkey). *Hydrogeol. J.*, 17, 2023 -2035. https://doi.org/10.1007/s10040-009-0497-0
USGS (2019). U.S. Geological Survey https://earlywarning.usgs.gov/ss

ebop/modis/8-day/608 (accessed September 24, 2020)

Wang, L., Butcher, A.S., Stuart, M.E., Gooddy, D.C. and Bloomfield, J.P. (2013). The nitrate time bomb - A numerical way to investigate nitrate storage and lag time in the unsaturated zone. *Environ. Geochem. Health*, 35(5), 667-81. https://doi.org/10.1007/s10653-013-9550-y

Water Quality Portal (WQP) (2019). National Water Quality Monitoring Council. https://www.waterqualitydata.us/portal/ (accessed August 12, 2020)

WHO (World Health Organization) (1995). *Guidelines for Drinking-Water Quality*, 2nd Ed. https://apps.who.int/iris/handle/10665/3855

Wohlgemuth, A. (2016). *Evaluating Groundwater Recharge in the Saloum Region of Senegal*. Open Access Master's Thesis, Michigan Technological University, Michigan, US

Yager, R.M. (1993). *Estimation of hydraulic conductivity of a riverbed and aquifer system on the Susquehanna River in Broome County, New York.* U.S. Geological water-supply paper; 2387, United States Government Printing Office, Washington.

Zhai, Y., Zhao, X., Teng, Y., Li, X., Zhang, J., Wu, J. and Zuo, R. (2017). Groundwater nitrate pollution and human health risk assessment by using HHRA model in an agricultural area, NE China. *Ecotoxicol. Environ. Saf.*, 137, 130-142. https://doi.org/10.1016/j.ecoenv.2016.11.010

Zhang, H., Yang, R., Wang, Y. and Ye, R. (2019). The evaluation and prediction of agriculture-related nitrate contamination in groundwater in Chengdu Plain, southwestern China. *Hydrogeol. J.*, 27, 785-799. https://doi.org/10.1007/s10040-018-1886-z

Zhang, H., Yang, R., Guo, S. and Li, Q. (2020). Modeling fertilization impacts on nitrate leaching and groundwater contamination with HYDRUS-1D and MT3DMS. *Paddy Water Environ.*, 18, 481-498. https://doi.org/10.1007/s10333-020-00796-6

Zheng, C. and Wang, P.P. (1999). MT3DMS: *A Modular Three-Dimensional Multispecies Transport Model for Simulation of Advection, Dispersion and Chemical Reactions of Contaminants in Groundwater Systems, Documentation and User's Guide.* Contract Report SERDP-99-1, U.S. Army Engineer Research and Development Center.